



Investigation of the Properties of PbS Thin Films Obtained by Chemical Bath Deposition Method at Relatively High pH

Ayça KIYAK YILDIRIM

Department of Motor Vehicles and Transportation Technologies, BilecikŞeyhEdebali University
BilecikŞeyhEdebali University,11210Bilecik/Turkey
ayca.kiyak@bilecik.edu.tr



ABSTRACT

Chemical bath deposition (CBD) method was used to deposit thin films of PbS. In the experiments, effects of pH deposition solution are examined on a scale of 11 to 13 in detail. The structural properties of the PbS films were examined by using X-ray diffractometer (XRD). According to the XRD, it was found that the intensity of the peaks increased and the crystallization of PbS thin films changed depending on the pH value of the deposition liquid. XRD results showed that the PbS film thickness increased with the increase in pH of the deposition liquid. Besides, crystallite sizes, lattice constants, average stresses, micro strains and dislocation densities were obtained from the XRD results. Although the films produced at pH 13, the micro strain and average stress of the film significantly increased. Also, the lattice parameters calculated are shifted. These results point out that the as acquired films were under strain. Surface images of the PbS samples were researched by using scanning electron microscope (SEM). The SEM images revealed that compact films surfaces were seen at low pH. On the other hand when PbS films were produced at high pH, there were clusters on the films surfaces.

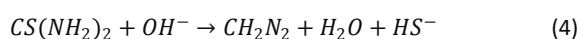
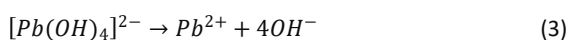
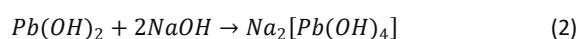
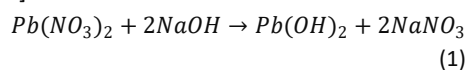
I Introduction

In recent years, interest in the development of semiconductor nanostructured materials has grown rapidly due to their unique physical and chemical properties [1]. This is because they have potential applications in areas such as solar cells, optoelectronic devices, photoconductors, sensor and infrared detector devices [2]. Its attractiveness is due to its low synthetic cost, its ability to handle solutions, its size, shape, doping and its dependence on optoelectronic properties such as surface chemistry [3-4]. Therefore, many studies have been reported on the form-controlled synthesis of semiconductor nanocrystals with different nanostructures [5-6].

For the past few years, the properties of PbS film for the research on the growth of nano

particle PbS films has increased. Owing to their suitable bandgaps, PbS thin films using solar control coatings [7], [8]. The use of very thin (20-60 nm) chemically deposited PbS films as solar control coatings has been debated with many researchers [9], [10]. In the literature, there are many different techniques research on preparing of PbS films such as spray pyrolysis [11], successive ionic layer adsorption and reaction [12], thermal evaporation [13], solid-vapor deposition [14], galvanic method [15], atomic layer deposition [16], pulse electrodeposition [17],[18], electrodeposition [19]-[23] microwave heating [24], and chemical bath deposition (CBD) [25]-[29] used to be produced Polycrystalline PBS. Within these methods, CBD is low cost method and the simplest experiment to produce thin films of PbS [29].

There are a few studies in the literature on PbS films grown on glass and other substrates at different pH by CBD. The effects of different pH scales have also been investigated, such as 11 to 13 by varying amount of NaOH[30] in this studies, lead acetate ($\text{Pb}(\text{CH}_3\text{COO})_2$), triethanolamine ($\text{C}_6\text{H}_{15}\text{NO}_3$), thiourea ($\text{SC}(\text{NH}_2)_2$) was used and 10 to 13 by varying amount of NaOH[31]. In this studies, Lead nitrate ($\text{Pb}(\text{NO}_3)_2$), thiourea ($\text{SC}(\text{NH}_2)_2$) was used. There are two studies related to produce of PbS in acidic bath such as 2.5, 5.0 and 6.0, but in mentioned studies [32], [33]. Mechanisms of PbS deposition reactions occurring during PbS film production by chemical bath precipitation are as follows. [25]:



II Procedure

Thin films deposition

Glass substrates of 5 cm x 2.5 cm x 2 mm were cleaned. The deposition liquid was prepared in 110 ml deionized water containing 0.0094 M lead nitrate [$\text{Pb}(\text{NO}_3)_2$], 0.0512 M thiourea ($\text{CS}(\text{NH}_2)_2$) and 0.33 M Thiourea [$\text{SC}(\text{NH}_2)_2$]. Alkalinity is adjusted using sodium hydroxide (NaOH). The glass substrates and the deposition bath were purged with 4.5% (w/w) hydrochloric acid and then washed with deionized water. The cleaned glass substrates were immersed vertically in the deposition bath. The pH values of all deposition liquids used in the production of PbS films were prepared to be 11, 11.5, 12, 12.5 and 13 respectively and pH of the solutions was adjusted by using dilute NaOH. All deposition liquids used during the production of PbS film were mixed at 550 rpm. PbS films were grown in 20 minutes. The temperature of the deposition liquid was maintained at room temperature (300 K) during the deposition process. After the film growth, the substrates were removed

from the deposition bath and they were rinsed in and double distilled water and dried in room conditions. Mirror-like smooth, dark brownish black thin film surfaces were obtained. One side of the glass substrates was deleted using HCL cotton.

Characterizations of thin films

The structural and morphological features of the PbS thin films were characterized. Film thickness was measured using Filmetrics F20 optical reflectometer. All film thicknesses were calculated by using gravimetric method. XRD analysis was performed using PANALIC EMPERJAN XRD in the range of 20° to 80° with 1.5°/min. Surface morphology of the prepared PbS thin films was investigated by using Zeiss SUPRA 40VP (SEM) scanning electron microscopy.

III. Results

A. Structural studies of PbS thin films

The crystal structure of PbS thin films produced using XRD technique such as crystal structure, crystallite size, preferential orientation, strain and stress acting on the unit surface were determined. The diffraction peaks observed at diffraction angles 2θ of 25.9°, 30°, 43°, 50.9°, 53.4°, 62.5° and 68.9° comply with the planes of the cubic PbS type structure (111), (002), (022), (113), (222), (004) and (133). PbS thin films produced at pH 11, 11.5, 12, 12.5 and 13 respectively (98-064-8453), (98-006-3095), (98-003-8293), (98-003-8293) and (98-006-3095) determined to be compatible with ASTM cards 006-2193. It was observed that the intensity of the peaks increased and the crystallization of PbS thin films changed depending on the pH value of the deposition liquid. XRD analyzes of PbS thin films produced at different pH values are given in Figure 1 and all films have been generated in cubic galena.

Film thicknesses were calculated using the gravimetric method and the results are given in Table 1. The thickness of the PbS films ranges between 300 nm and 850 nm. This result showed that the PbS film thickness increased with the increase in pH of the deposition liquid. The pH of the solutions admixture was effected by OH^- amount and it might have an influence on the reaction rate as indicated by A. Antony et al [34]. The alkaline medium of the final solution in that case helps to decomposition thiourea with the release of S^{2-}

² amounts [35]. In a previous study, the thickness of obtained ZnS samples increases with increasing pH [30]. In order to same deposition durations, films deposited at relatively low pH result in more thin films, while films fabricated at relatively high pH result in more thick films. This effect is probably resulted from the lack of thiourea decomposition at low pH [30].

The texture coefficients, given in Equation 7 [36], of the films were utilized to definition of preferred orientation.

$$TC = \frac{I_{(hkl)}/I_{0(hkl)}}{\frac{1}{N} \sum_N \left(\frac{I_{(hkl)}}{I_{0(hkl)}} \right)} \quad (7)$$

where $I(hkl)$ is the measured relative intensity of a plane (hkl), $I_0(hkl)$ is the standard intensity of the plane (hkl) given in ASTM card. The calculated texture coefficients were given in Table 1. It has been determined that all films have 3 texture coefficient values larger than 1 belonging to different planes. The preferred orientation for all films produced is thought to be random. According to the texture coefficients although the films produced at 11 pH, the peak intensity of (002) plane of the film was significantly higher than that of the (111) plane. This result is an expected result because of the fact that pH of the final solutions admixture depends on OH^{-1} concentration. So they might have an influence on the film reaction rate. Due to this reason, the peak intensity of (111) plane of the film can be expected to shift towards the (002) plane.

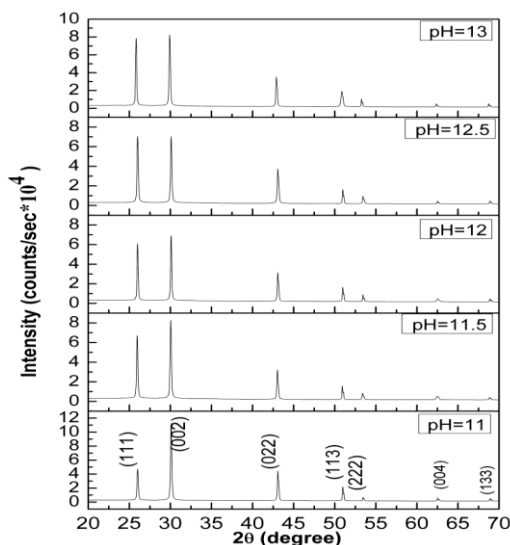


Fig.1 X-ray diffractograms of PbS thin films according to deposition time

Debye Scherrer equation given in Equation 8 was used to estimate the average crystallite sizes of PbS films

$$cs = \frac{0.089 * 180 * \lambda}{314 * \beta * \cos \theta_c} \text{ nm} \quad (8)$$

where λ was the wavelength of X-ray radiation (1.54056 Å), $2\theta_c$ was the peak centre and β was the full width half maximum. β and $2\theta_c$ were calculated by fitting the XRD peak profile [37]. The estimated average crystallite sizes of the films were given in Table 2. When Table 2 is pursued, it can be seen that average crystallite size varies from 53 nm to 93 nm. The lattice constant of the cubic rock salt structure is given as follows by [38].

$$a = d \sqrt{h^2 + k^2 + l^2} \quad (9)$$

where h, k and l are the Miller indices and d is the interplanar distance. Moreover, the average stress and micro strain using Equations 10 and 11, respectively, were calculated and are given in Table 2.

$$\varepsilon = (a_0 - a)/a_0 \quad (10)$$

$$S = \varepsilon Y / (2\sigma) \quad (11)$$

where a_0 and a are lattice parameter of the bulk sample and the corrected value of lattice parameter of thin film samples respectively. The σ and Y are the Poisson's ratio and Young's modulus of the bulk crystal respectively. For PbS the value of Y is 70.2 GPa and σ is 0.28. The corrected values are anticipated from the Nelson–Riley plots demonstrated in Fig,2, Fig,3, Fig,4 and Fig,5. The lattice parameters calculated from the peak positions of individual reflections are plotted against $F(\theta)$ and the intercept of the linear plot at gives the corrected lattice constant strain using Equations 12 and 13, respectively [39].

$$F(\theta) = (\cos^2 \theta / 2) * \left(\frac{1}{\sin^2 \theta} + \frac{1}{\theta} \right) \quad (12)$$

$$(\cos^2 \theta / 2) * \left(\frac{1}{\sin^2 \theta} + \frac{1}{\theta} \right) = 0 \quad (13)$$

Deviation of the calculated lattice parameter (a) from the strain face bulk sample ($a_0 = 5.936$ nm) point outs that the as acquired films were under strain [39].

Dislocation density can be derived from the crystallite size as given in Equation 13 realized in Table 2 [40]

$$\delta = \frac{1}{(cs)^2} \quad (12)$$

According to Table 2 although the films produced at pH 13, the micro strain and average stress of the film significantly increased. Also, Nelson–Riley plots of PbS thin films obtained at pH 13 demonstrated in Fig.5. The lattice parameters calculated are shifted. These results point out that the as acquired films were under strain [39].

Table 1. The intensity, texture coefficient, and film thickness of the PbS thin films produced at pH 11, 11.5, 12, 12.5 and 13

EXPERIMENT	2θ	INTENSITY (COUNT/ SECONDS)	I / I ₀	TC	(hkl)	FILM THICKNESS (nm)
E1	25,993	46445,59	38,98	1,22	(111)	322
	30,075	108743	100	3,13	(002)	
	43,075	44934,57	45,3	1,42	(022)	
	50,979	22043,06	23,5	0,74	(113)	
	53,449	6880,51	6,11	0,19	(222)	
	62,523	5924,531	5,28	0,17	(004)	
	68,919	5441,547	4,61	0,14	(133)	
E2	25,967	67027,73	77,71	2,43	(111)	451
	30,049	82942,11	100	3,13	(002)	
	43,023	31940,65	43,44	1,36	(022)	
	50,927	15581,01	21,98	0,69	(113)	
	53,423	7499,314	10,34	0,32	(222)	
	62,523	5089,826	4,78	0,15	(004)	
	68,893	3876,309	4,35	0,14	(133)	
E3	25,993	60949,39	81,63	2,55	(111)	656
	30,075	67943,27	100	3,13	(002)	
	43,075	31506,47	49,56	1,55	(022)	
	50,979	16481,67	26,64	0,83	(113)	
	53,423	8807,722	12,51	0,39	(222)	
	62,523	4742,04	5,09	0,16	(004)	
	68,893	4642,981	5,78	0,18	(133)	
E4	25,993	69906,43	97,26	3,04	(111)	837
	30,075	66945,2	100	3,13	(002)	
	43,075	37451,27	58,38	1,83	(022)	
	50,979	16419,11	27,68	0,87	(113)	
	53,449	9373,405	14,2	0,44	(222)	
	62,523	4347,918	5,43	0,17	(004)	
	68,893	4611,198	5,78	0,18	(133)	
E5	25,915	40002,18	98,27	3,07	(111)	858
	30,023	43186,24	100	3,13	(002)	
	43,023	20038,46	49,62	1,55	(022)	
	50,901	18069,31	23,82	0,75	(113)	
	53,423	6076,849	14,11	0,44	(222)	
	62,549	3420,15	5,81	0,18	(004)	
	68,919	3261,558	5,9	0,18	(133)	

Table 2. The crystalite size, dislocation densities, lattice parameter, micro strain values, and average stress values of the PbS thin films produced at pH 11, 11.5, 12, 12.5 and 13

EXPERIMENT	2θ	CRYSTALITE SIZE (nm)	LATICE PARAMETER A (VERIFIED) (Å)	MİKRO STRAIN *10 ⁻³	DISLOCATION DENSITY (lines/m ²)*10 ⁻⁴	AVERAGE STRESS (10 ⁸ N/m ²)
pH=11	25,993	53	5,9377	2,86	3,63	0,36
	30,075	53	5,9422	10,4	3,56	1,31
	43,075	66	5,9406	7,80	2,30	0,98
	50,979	85	5,9411	8,65	1,38	1,08
	53,449	86	5,9393	5,57	1,35	0,70
	62,523	90	5,9416	9,43	1,24	1,18
	68,919	93	5,9390	4,98	1,15	0,62
pH=11.5	25,967	53	5,9448	14,8	3,63	1,85
	30,049	53	5,9478	19,9	3,56	2,50
	43,023	66	5,9448	14,8	2,30	1,86
	50,927	85	5,9446	14,5	1,38	1,81
	53,423	69	5,9429	11,6	2,12	1,46
	62,523	36	5,9442	13,7	7,75	1,72
	68,893	74	5,9416	9,46	1,80	1,19
pH=12	25,993	63	5,9739	5,04	2,52	0,63
	30,075	64	5,9717	10,8	2,47	1,36
	43,075	66	5,9612	9,47	2,30	1,19
	50,979	85	5,9542	9,66	1,38	1,21
	53,423	86	5,9556	7,67	1,35	0,96
	62,523	45	5,9536	11,4	4,97	1,43
	68,893	93	5,9509	7,18	1,15	0,90
pH=12.5	25,993	53	5,9390	3,38	3,63	0,42
	30,075	53	5,9424	9,16	3,56	1,15
	43,075	55	5,9416	8,85	3,31	1,11
	50,979	85	5,9417	9,1	1,38	1,14
	53,449	69	5,9406	7,03	2,12	0,88
	62,523	90	5,9428	9,57	1,24	1,20
	68,893	74	5,9403	7,7	1,83	0,97
pH=13	25,915	63	5,9380	63,8	2,52	8,00
	30,023	53	5,9414	60,2	3,57	7,54
	43,023	66	5,9413	42,4	2,30	5,31
	50,901	42	5,9414	30,7	5,54	3,84
	53,423	86	5,9402	33	1,36	4,14
	62,549	90	5,9417	29,6	1,24	3,71
	68,919	93	5,9406	25	1,16	3,14

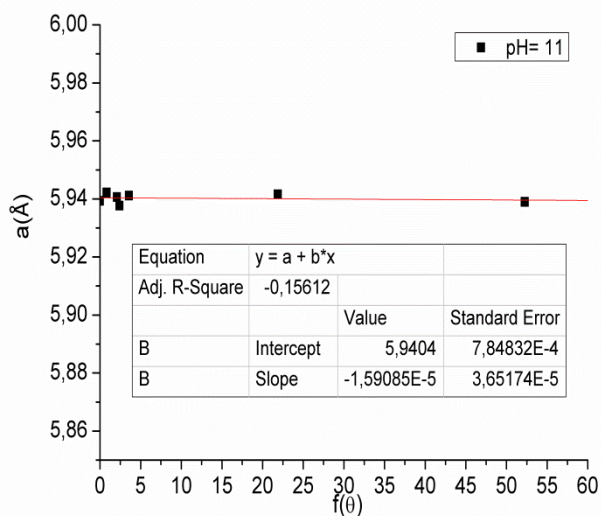


Fig.1 Nelson–Riley plots of PbS thin films obtained at pH 11

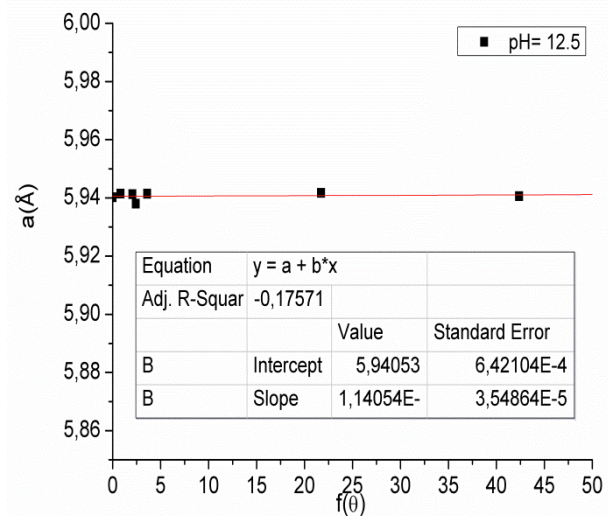


Fig.4 Nelson–Riley plots of PbS thin films obtained at pH 12.5

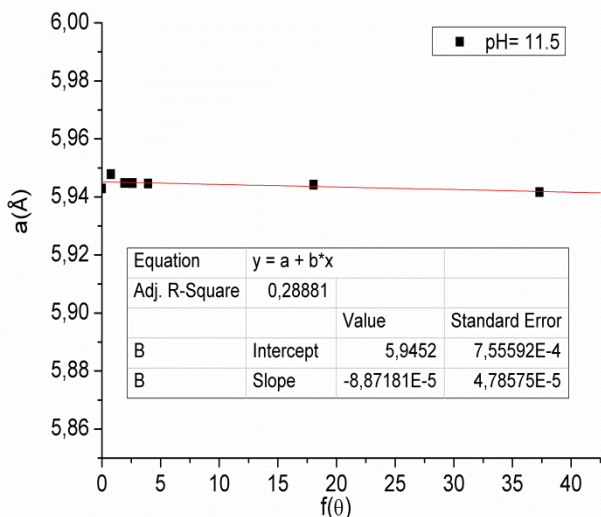


Fig.2 Nelson–Riley plots of PbS thin films obtained at pH 11.5

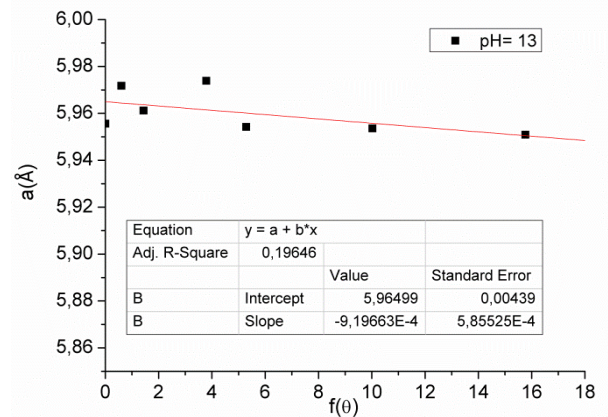


Fig.5 Nelson–Riley plots of PbS thin films obtained at pH 13

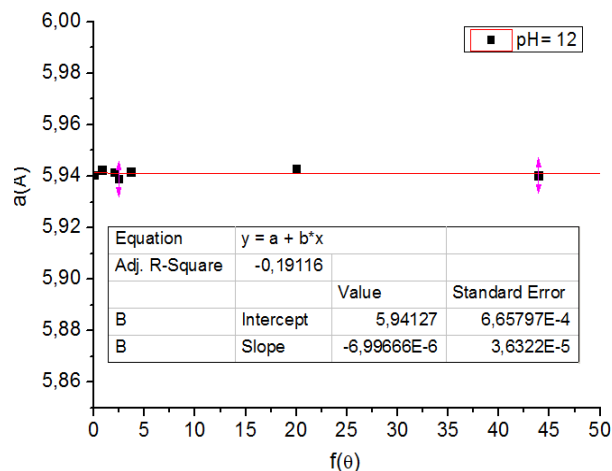


Fig.3 Nelson–Riley plots of PbS thin films obtained at pH 12

Surfaces of PbS thin films

Typical 100 times magnified SEM images were demonstrated in Fig.6 and Fig.7. There are plenty of voids and pinholes on the surface of the films obtained with pH 12.5 and 13 demonstrated in Fig.7b and Fig.7c respectively. It is thought that increasing deposition solution pH increased pinholes and voids formations as given in Figure 7b, and 7c. The 20000 times magnified surface images were shown in Fig.8 and Fig.9. The films obtained at pH11, 11.5 and 12 given in Fig.8a, Fig.8b and Fig.8c respectively. These PbS films surfaces are seen typical polymorphic morphology. The sizes of the polymorphic particles range 150 nm to 800 nm. It is considerable that there are not pinholes and voids on these surfaces. This result is realized that

relatively high SEM images can be misleading for people.

Homogeneous PbS films were observed at relatively low pH were demonstrated in Fig.6. Relatively high Pb^{2+} amounts in the deposition solution is anticipated owing to lower complexation of the Pb^{2+} ions at low pH; nevertheless, the lower hydrolysis of the thiourea also limits the concentration of S^{2-} free ions. It is resulted in more thin films.

PbS samples obtained at relatively high pH values have compact surfaces, but it was seen clusters at the PbS surface. This formation may be resulted from high reaction rate at higher pH. At high pH the Pb^{2+} amounts is more low through increase pH higher complexation, but S^{2-} amounts is higher and results in higher reaction rates.

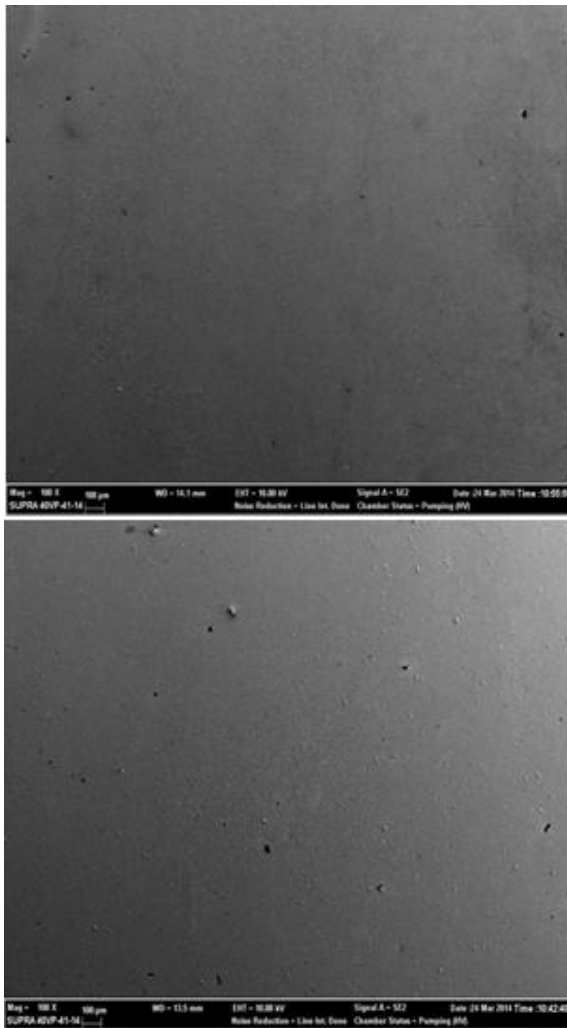


Fig.6 SEM images of the PbS films obtained at pH a)11& b) 11.5 magnified 100 times.

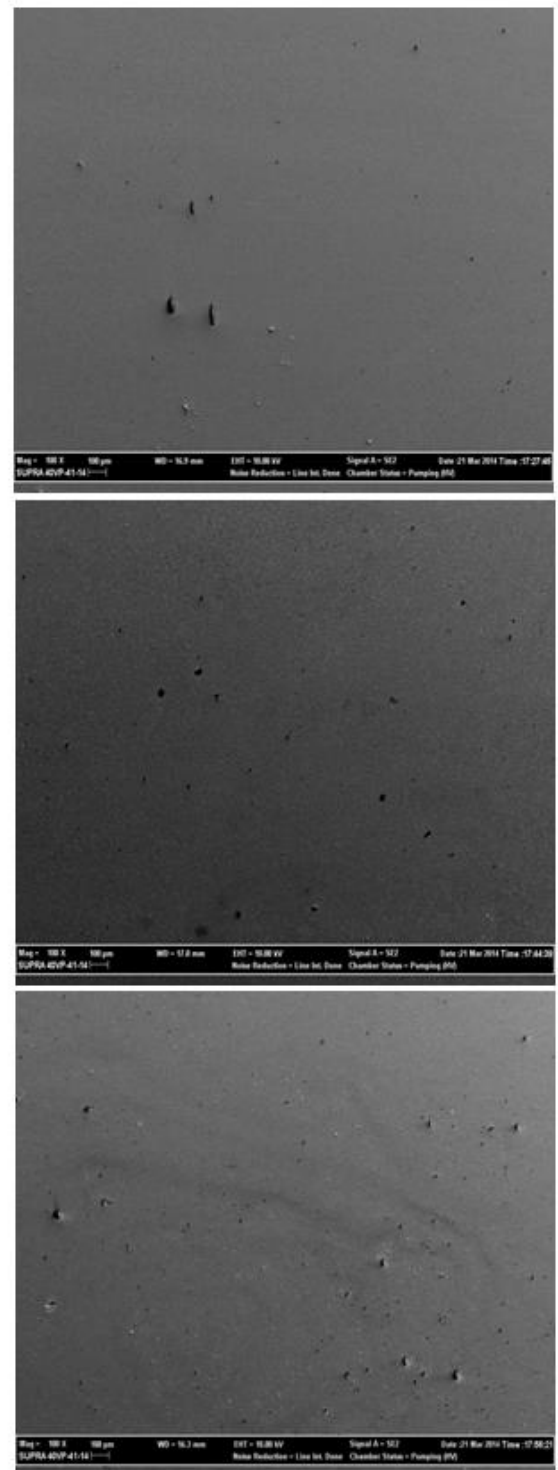


Fig.7 SEM images of the PbS films obtained at pH a) 12, b) 12.5 c)13 magnified 100 times

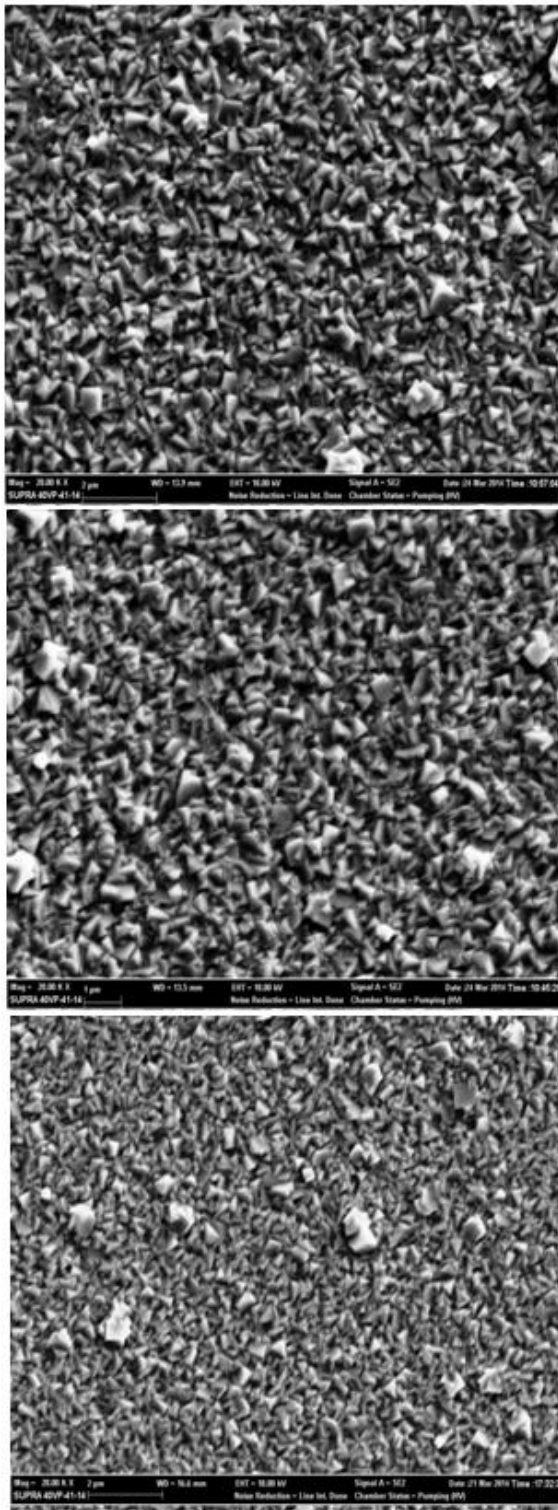


Fig.8 SEM images of the PbS films obtained at pH a)11, b) 11.5, c) 12 magnified 20000 times

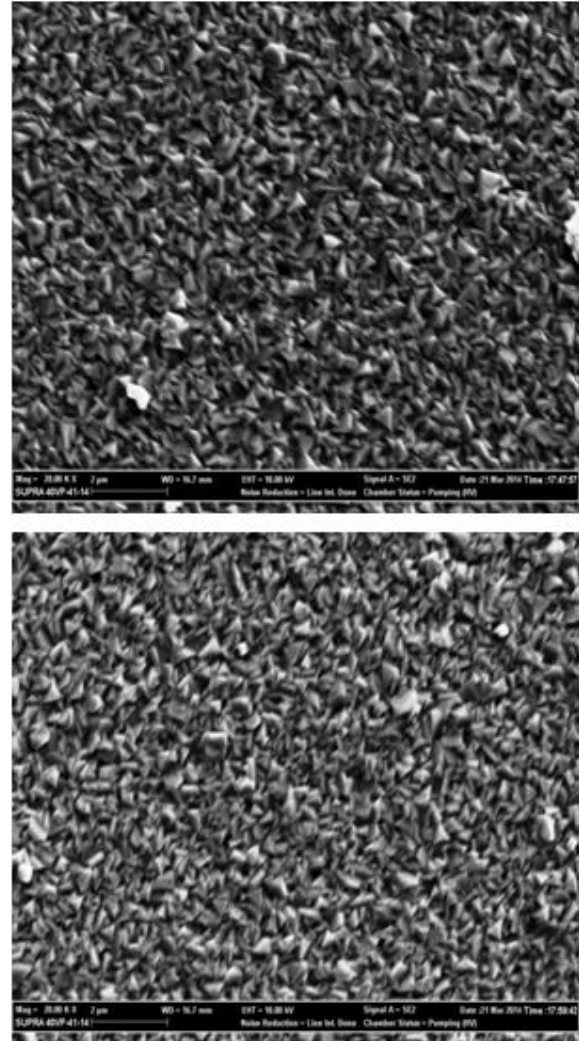


Fig.9 SEM images of the PbS films obtained at pH a)12.5 b) 13 magnified 20000times

IV. CONCLUSIONS

In this work, PbS samples were growth by chemical bath deposition. Five different pH of deposition solution were used in the experiments. XRD data showed that the intensity of the peaks increased and the crystallization of PbS thin films changed depending on the pH value of the deposition liquid. All PbS films formed in cubic galena structure. XRD results showed that the PbS film thickness increased with the increase in pH of the deposition liquid. The pH of the final solutions admixture depends on OH^{-1} concentration and might have an influence on the film growth rate as indicated by A. Antony et al [34]. According to the texture coefficients although the films produced at 11 pH, the peak intensity of (002) plane of the film was significantly higher than that of the (111) plane.

This result is an expected result because of the pH of the final solutions depends on OH^{-1} concentration.

Although the films produced at pH 13, the micro strain and average stress of the film significantly increased. Also, the lattice parameters calculated are shifted. These results point out that the as acquired films were under strain [39].

The surface morphologies were investigated by using a SEM device and the SEM images showed that homogeneous PbS films was fabricated at relatively low pH and PbS samples obtained at relatively high pH values are compact films, but it is seen clusters at the PbS surface. At low pH, it was resulted relatively high Pb^{2+} ions in the deposition solution is anticipated owing to lower complexation of the Pb^{2+} ions; nevertheless, the lower hydrolysis of the thiourea also limits the concentration of S^{2-} free ions. This causes thinner films. At relatively high pH, the Pb^{2+} ions concentration is lower through Increase pH higher complexation, but S^{2-} free ions concentration is higher and results in higher deposition rates.

REFERENCES

- [1]. Y. N. Xia, P. D. Yang, Y. G. Sun, Y. Y. Wu, B. Mayers, B. Gates, Y. D. Yin, F. Kim, Y. Q. Yan, *Adv. Mater.*, 15, 353-389, (2003).
- [2]. H. Karami, M. Ghasemi, S. Matini, *Int. J. Electrochem. Sci.*, 8 11661-11679, (2013)
- [3]. S. C. Erwin, L. Zu, M. I. Haftel, A. L. Efros, T. A. Kennedy, D. J. Norris, *Nature*. 436 (2005) 9194.
- [4]. X. G. Peng, L. Manna, W. D. Yang, J. Wickham, E. Scher, A. Kadavanich, A. P. Alivisatos, *Nature*. 404 (2000) 59
- [5]. Y. Peng, A. W. Xu, B. Deng, M. Antonietti, H. Cölfen, *J. Phys. Chem. B*. 110 (2006) 2988.
- [6]. Oshero, A., Makai, J., Balazs, J., Horvath, Z., Gutman, N., Sa'ar, A. and Golan, Y. (2010). Tunability of the optical band edge in thin PbS films chemically deposited on GaAs(100). *Journal of Physics: Condensed Matter*, 22(26), p.262002.
- [7]. Nair, P., Garcia, V., Hernandez, A. and Nair, M. (1991). Photoaccelerated chemical deposition of PbS thin films: novel applications in decorative coatings and imaging techniques. *Journal of Physics D: Applied Physics*, 24(8), pp.1466-1472.
- [8]. Espevik, S., Wu, C. and Bube, R. (1971). Mechanism of Photoconductivity in Chemically Deposited Lead Sulfide Layers. *Journal of Applied Physics*, 42(9), pp.3513-3529.
- [9]. Nair, P., Nair, M., Fernandez, A. and Ocampo, M. (1989). Prospects of chemically deposited metal chalcogenide thin films for solar control applications. *Journal of Physics D: Applied Physics*, 22(6), pp.829-836.
- [10]. Thiagarajan, R., MahaboobBeevi, M., Anusuya, M. and Ramesh, T. (2012). Influence of reactant concentration on nano crystalline PbS thin films prepared by Chemical Spray Pyrolysis. *Optoelectronics and Advanced Materials – Rapid Communications*, 6(1), pp.132-135.
- [11]. Kanninen, T., Lindroos, S., Resch, R., Leskelä, M., Friedbacher, G. and Grasserbauer, M. (2000). Structural and topographical studies of SILAR-grown highly oriented PbS thin films. *Materials Research Bulletin*, 35(7), pp.1045-1051..
- [12]. Ibrahim, A. (2009). Structure and electronic properties of evaporated thin films of lead sulfide. *Defect and Diffusion Forum*, 294, pp.85-92.
- [13]. Obaid, A., Mahdi, M. and Zainuriah, H. (2012). Growth of nanocrystalline PbS thin films by solid-vapor deposition. *Advanced Materials Research*, 620, pp.1-6.
- [14]. Mondal, A. and Mukherjee, N. (2006). Cubic PbS thin films on TCO glass substrate by galvanic technique. *Materials Letters*, 60(21-22), pp.2672-2674.
- [15]. Dasgupta, N., Lee, W. and Prinz, F. (2009). Atomic layer deposition of lead sulfide thin films for quantum confinement. *Chemistry of Materials*, 21(17), pp.3973-3978.
- [16]. Mathews, N., Ángeles-Chávez, C., Cortés-Jácome, M. and Toledo Antonio, J. (2013). Physical properties of pulse

- electrodeposited lead sulfide thin films. *Electrochimica Acta*, 99, pp.76-84.
- [17]. Thirumoorthy, P. and Murali, K. (2010). Characteristics of pulse electrodeposited PbS thin films. *Journal of Materials Science: Materials in Electronics*, 22(1), pp.72-76.
- [18]. KiyakYildirim, A. and Altıokka, B. (2017). An investigation of effects of bath temperature on CdO films prepared by electrodeposition. *Applied Nanoscience*. doi: 10.1007/s13204-017-0591-x
- [19]. KiyakYildirim, A. and Altıokka, B. (2017). Effects of concentration on CdO films grown by electrodeposition. *Applied Nanoscience*. 7:131–135. doi:10.1007/s13204-017-0552-4
- [20]. Altıokka, B. and KiyakYildirim, A. (2015). Effects of external alternating magnetic field on ZnO films obtained by electrodeposition. *Arabian Journal for Science Engineering*. doi: 10.1007/s13369-015-1980-7
- [21]. Altıokka, B. and KiyakYildirim, A. (2018). Effects of pH on CdO films deposited onto ITO coated glass substrates by electrodeposition. *Int. J. Surface Science and Engineering*, 12(1), pp.13-22.
- [22]. Altıokka, B. and KiyakYildirim, A. (2018). Electrodeposition of CdS Thin Films at Various pH Values. *Journal of the Korean Physical Society*, 72(6), pp.687-691.
- [23]. Zhao, Y., Liao, X., Hong, J. and Zhu, J. (2004). Synthesis of lead sulfide nanocrystals via microwave and sonochemical methods. *Materials Chemistry and Physics*, 87(1), pp.149-153.
- [24]. Altıokka, B., Baykul, M., Altıokka, M., 2013. Some physical effects of reaction rate on PbS thin films obtained by chemical bath deposition. *Journal of Crystal Growth*, 384, pp.50-54.
- [25]. Altıokka, B., 2015. Effects of Inhibitor on PbS Thin Films Obtained by Chemical Bath Deposition. *Arabian Journal for Science and Engineering*, 40(7), pp.2085-2093.
- [26]. Valenzuela-Jáuregui, J., Ramírez-Bon, R., Mendoza-Galván, A. and Sotelo-Lerma, M. (2003). Optical properties of PbS thin films chemically deposited at different temperatures. *Thin Solid Films*, 441(1-2), pp.104-110.
- [27]. Pentia, E., Pintilie, L., Matei, I. and Pintilie, I. (2001). Field Effect Controlled Photoresistors Based on Chemically Deposited PbS Films. *MRS Proceedings*, 692.
- [28]. Kumar, S., Sharma, T., Zulfequar, M. and Husain, M. (2003). Characterization of vacuum evaporated PbS thin films. *Physica B: Condensed Matter*, 325, pp.8-16.
- [29]. Kumar, S., Sharma, T., Zulfequar, M. and Husain, M. (2003). Characterization of vacuum evaporated PbS thin films. *Physica B: Condensed Matter*, 325, pp.8-16.
- [30]. Carrillo-Castillo, A., Aguirre-Tostado, F. S., Salasvillasenor A., Mejia, I., Gnade, B. E., Sotelo-Lerma, M. and Quevedo-López, M.A. (2013). Effect Of Chemical Bath Deposition Parameters On The Growth Of PbS Thin Films For TFTS Applications. *Chalcogenide Letters*, Vol. 10(3), pp.105–111.
- [31]. Mousa, A. M., Hassen, S. M., and Mohmoed, S. (2014). Effect of deposition parameters on kinematics growth and optical properties of PbS nano films deposited by chemical bath deposition. *International Letters of Chemistry, Physics and Astronomy*, Vol. 15, pp.1–10.
- [32]. Gadave, K.M., Jodgudri, S.A. and Lokhande, C.D. (1994). Chemical deposition of PbS from an acidic bath. *Thin Solid Films*, Vol. 245, pp.7–9.
- [33]. Soonmin, H.O. Kassima, A. Weetee, T. (2013). The role of Bath Temperature in aqueous Acidic Chemically PbS Films. *Journal of Basic and Applied Scientific Research*, Vol. 3(11), pp.353-357.
- [34]. Antony, K.V. Murali, R. Manoj, M.K. Jayaraj, Materials Chemistry and Physics 90, 106 (2005).
- [35]. V. Stancu, M. Buda, L. Pintilie, T. Botila, G. Iordache, *Thin Solid Films* 516, 4301 (2008).

- [36]. Devi, R., Purkayastha, P., Kalita, P. and Sarma, B. (2007). Synthesis of nanocrystalline CdS thin films in PVA matrix. Bulletin of Materials Science, 30(2), pp.123-128.
- [37]. Guo, R., Liang, Y., Gao, X., Zhu, H., Zhang, S. and Liu, H. (2014). Microstructure and Near Infrared Absorption of PbS Films Deposited by Chemical Bath Deposition on p-Type Si(100) Wafers. Brazilian Journal of Physics, 44(6), pp.697-702.
- [38]. Soetedjo, H., Aziz, B., Aziz, I., Sudjatmoko, S., 2017. Low resistivity of Cu and Fe doped PbS thin films prepared using dc sputtering technique,. Journal of Non-Oxide Glasses, 9, pp.55–63.
- [39]. Bhowmik, R.N., NrisimhaMurthy, M. and SekharSrinadhu, E. (2008) 'Magnetic modulation in mechanical alloyed Cr_{1.4}Fe_{0.6}O₃ oxide' PMC Physics B, Vol. 1, pp.20–38.
- [40]. Hussain, A., Begum, A., Rahman, A., 2012. Characterization of Nanocrystalline Lead Sulphide Thin Films Prepared by Chemical Bath Deposition Technique. Arabian Journal for Science and Engineering, 38(1), pp.169-174.